Influence of growth conditions on structural parameters of scheelite PbTO$_4$ (T = Mo, W) crystals

I.A. Kaurova [a,*], G.M. Kuz'micheva [a], A.A. Brykovskiy [a], V.B. Rybakov [b], Yu.N. Gorobets [c], A.N. Shekhovtsov [c], A. Cousson [d]

[a] Department of Materials Science and Technology of Functional Materials and Structures, Moscow Technological University, MITHT, Vernadskogo pr. 86, Moscow 119571, Russia
[b] Department of Chemistry, Lomonosov State University, Vorobyovy Gory, Moscow 119992, Russia
[c] Department of Ferroelectric and Laser Single Crystals, Institute for Single Crystals of NAS of Ukraine, Lenin 60, Ave., Kharkov 61001, Ukraine
[d] Laboratoire Leon Brillouin, Cea/Saclay, Gif-sur-Yvette Cedex 91191, France

ARTICLE INFO

ABSTRACT

Lead molybdates and tungstates with general chemical formula PbTO$_4$ (PTO), where T is Mo (PMO) or W (PWO), were grown by the Czochralski method in an oxygen (PTO-A) or inert (PTO-N$_2$) atmosphere from a stoichiometric mixture of corresponding oxides or mixture containing an excess of PbO (PMO-N$_2$(Pb)). The crystals were investigated by X-ray and neutron single crystal and X-ray powder (Rietveld method) diffraction methods. For PWO-A and PWO-N$_2$ crystals, the presence of additional reflections (50%) was revealed, indicating the symmetry reduction from space group $I4_1/a$ to $I\bar{4}$ caused by kinetic (growth) order–disorder phase transition associated with an ordering/disordering of oxygen vacancies. In the structures of PMO samples, the vacancies are absent in the Mo and O sites (PMO-A and PMO-N$_2$) and they are present in the Pb sites (except for PMO-N$_2$(Pb)); the defect content being higher in the PMO-N$_2$ crystal grown in an inert atmosphere. It is shown that the light yellow color of PTO crystals is due to the O and Pb vacancies, that may be accompanied by the transition Pb^{2+} → Pb^{3+}, and the gray-purple color of PMO-N$_2$(Pb) is due to the transition Mo^{6+} → Mo^{5+}.

© 2016 Elsevier Ltd. All rights reserved.

1. Introduction

Lead molybdates PbMoO$_4$ (PMO) and tungstates PbWO$_4$ (PWO) with the general chemical formula PbTO$_4$ (T = Mo, W) (PTO) are related to optical materials belonging to the crystal family with scheelite-type structure (CaWO$_4$, space group $I4_1/a$, $Z = 4$) [1]. In PbTO$_4$ structure, Pb atoms are located in PbO$_8$ dodecahedra (square antiprism with refracted upper faces; the symmetry of dodecahedron is S_4) with coordination number (CN) $- 4 + 4$, i.e., with two sets of different cation-anion interatomic distances ($d_{A1-O} > d_{A2-O}$, Å). The PbO$_8$ polyhedra communicate with each other by the edges, each dodecahedron being surrounded by four neighboring PbO$_8$-dodecahedra. The PbO$_8$ dodecahedra and TO$_4$ tetrahedra (CN = 4; the symmetry of tetrahedron is S_4) are connected via a common vertices. The PbTO$_4$ structure is characterized by a specific law of cation alternation: the chess ordering of Pb and T atoms is observed in planes parallel to the refracted faces of dodecahedra (Fig. 1a). Each O atom is coordinated, in turn, by two Pb atoms and one T atom (CN = 3).

PTO crystals are promising materials for various applications due to their unique functional properties. PMO crystal is one of the most efficient material used in acousto-optical devices, such as modulators, deflectors and phase shifters, due to its low optical losses, high optical homogeneity and stability of laser emission [2], whereas PWO crystal, with low decay time, high density, and radiation resistance, is of practical use in electromagnetic detectors in high-energy accelerators used for high-energy physics research at CERN [3]. PTO crystals have attracted significant interest recently due to their possible use as a scintillation (cryogenic) detectors for rare event (for example, double β decay of ^{180,186}W и ^{92,98,100}Mo) and dark matter searches [4–6].

Czochralski method for growing crystal by its pulling from melt on a seed is usually used to produce single crystals with scheelite-type structure. This method allows to obtain bulk crystals with different dopants at a sufficiently high rate, and makes it possible to monitor the growth process. The majority of studies are devoted to molybdates as they grow better at lower temperatures compared with tungstates [7–12].

PMO crystals are usually grown from a charge obtained by solid phase synthesis of PbO and MoO$_3$ oxides taken in a stoichiometric ratio (e.g., [2,10,11]). Takano et al. [12] describes the main parameters of PMO single crystal growth by the Czochralski method: the charge, PbO and MoO$_3$ (99.99% purity) equimolar mixture; the crucible, Pt or Ir; the average crucible rotation rate, ~50 rev/min; the crystal pulling rate, ~5 mm/h; the cooling rate, ~60°/h; the temperature fluctuation

* Corresponding author at: Department of Materials Science and Technology of Functional Materials and Structures, Moscow Technological University, MITHT, 86 Vernadsky pr., Moscow 119571, Russia.
E-mail address: kaurchik@yandex.ru (I.A. Kaurova).
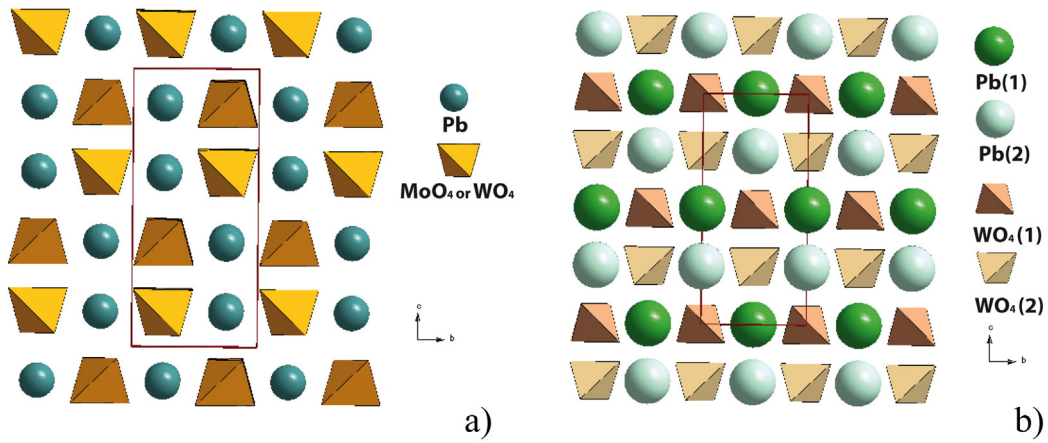
Fig. 1. Structure of $PbTO_4$ (T = Mo, W) (space group $I4_1/a$) (a) and $PbWO_4$ (space group $I\bar{4}$) (b) crystals.

Table 1
Characteristics of the samples under investigation.

Designation	Description	Color
PMO-A	$PbMoO_4$ growth in air atmosphere, annealing in vacuum atmosphere	Light yellow transparent
PMO-N_2	$PbMoO_4$ growth in N_2 atmosphere, annealing in vacuum atmosphere	Light yellow transparent
PMO-N_2(Pb)	$PbMoO_4$ excess of PbO in initial charge composition, growth in N_2 atmosphere, annealing in vacuum atmosphere	Gray-purple transparent
PWO-A	$PbWO_4$ growth in air atmosphere, annealing in vacuum atmosphere	Light yellow transparent
PWO-N_2	$PbWO_4$ growth in N_2 atmosphere, annealing in vacuum atmosphere	Light yellow transparent

during the crystal growth, 0.3 °C; the growth atmosphere, an air or Ar; the pressure, 1 atm. High homogeneity (without grains) and transparency of as-grown PMO single crystals were achieved by using $PbMoO_4$ seed with orientation ⟨001⟩. Refinement of crystal structure of as-grown crystals was not carried out.

According to [10], the yellow color of PMO crystals is caused by the anti-site point defects (the presence of Pb ions in Mo sites − $Mo^{n\bullet}_{Pb}$) or by the charge exchange, $Pb^{2+} + Mo^{6+} \rightleftarrows Pb^{3+} + Mo^{5+}$, of the cations. According to [13], the coloration is due to the associates of point defects, i.e., vacancies in the Mo or Pb sites and localized holes, $(V^{n'}_{Mo},nh^\bullet)^x$ or $(V^{n'}_{Pb},nh^\bullet)^x$, respectively.

According to [14], the yellow-colored PMO crystals, grown by the Czochralski method in Pt crucible in an inert atmosphere, had vacancies in the Mo sites ($V^{n'}_{Mo}$) (according to the single crystal and powder X-ray diffraction analyses of microparts and samples ground to a powder, respectively) and, possibly, vacancies in the O sites ($V^{n\bullet}_O$) (according to the single-crystal Neutron Diffraction Analysis of crystal macroparts).

PWO crystals are more fragile than PMO ones: they are prone to cracking and chipping from the seed during the Czochralski growth, which complicates the synthesis of bulk single crystals. According to [15], the use of $CaWO_4$ crystal with orientation <104> as a seed provided the growth of homogeneous PWO single crystal without cracks. Oeder et al. [15] suggested that the Czochralski growth of PTO crystals using Pt crucible results in yellow color of as-grown crystals (the appearance of the absorption band near 425 nm (2.9 eV)). According to [15], the oxygen vacancies ($V^{n\bullet}_O$) cannot be a color centers and the coloration of PWO depends on the contamination from Pt crucible. In addition, the yellow coloration may also be due to the oxidizing atmosphere, as evidenced by the obtaining of colorless crystal in Ir crucible in Ar atmosphere [15]. The influence of crystal growth atmosphere (air and argon) on the color centers in PWO single crystals has been investigated by Kim et al. [16]: when the PWO crystals were grown in air atmosphere, they exhibit a yellowish tint with additional spectral responses around 2.9 and 3.5 eV as compared with the colorless crystals grown in argon. As a result, it was assumed that yellow color is due to
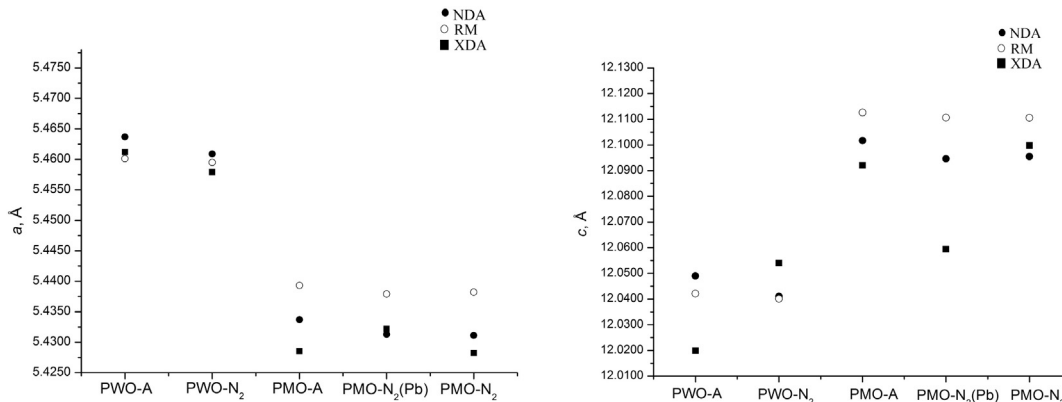
Fig. 2. The unit cell parameters of $PbMoO_4$ and $PbWO_4$ samples according to the NDA, XDA and RM data.

Table 2
Crystallographic data, experimental details and parameters of PbMoO$_4$ crystal structure refinement according to the NDA and XDA data.

Chemical formula of the nominal composition	PbMoO$_4$				
System, space group, Z	Tetragonal, $I4_1/a$, 4				
Technique	NDA		XDA		
Sample	PMO-N$_2$	PMO-N$_2$(Pb)	PMO-A	PMO-N$_2$	PMO-N$_2$(Pb)
a, Å	5.4311(1)	5.4313(1)	5.4285(2)	5.4282(5)	5.4322(2)
c, Å	12.0946(2)	12.0952(2)	12.0921(7)	12.059(1)	12.0998(8)
V, Å^3	356.75(2)	356.81(2)	356.34(2)	355.34(2)	357.05(2)
D_x, g/cm^3	6.836	6.835	6.843	6.863	6.830
Radiation λ, Å	0.828		Mo K_α; 0.71073		
Absorption μ, mm^{-1}	0.01		50.55	50.69	50.45
T, K	293				
Sample size, mm	~5 × 5 × 5		~0.1 × 0.1 × 0.1		
Diffractometer	5C2		STOE Stadi Vari PILATUS 100 K		
Type of scan	ω				
θ_{max}, deg.	42.500	42.800	30.915	30.545	30.835
Limits h, k, l	$0 \leq h \leq 8$	$-8 \leq h \leq 8$	$-7 \leq h \leq 7$	$-7 \leq h \leq 7$	$-7 \leq h \leq 7$
	$-8 \leq k \leq 8$	$-4 \leq k \leq 8$	$-7 \leq k \leq 7$	$-7 \leq k \leq 3$	$-7 \leq k \leq 6$
	$0 \leq l \leq 19$	$-11 \leq l \leq 19$	$-17 \leq l \leq 17$	$-17 \leq l \leq 17$	$-14 \leq l \leq 17$
Number of reflections measured/number of unique reflections/number of reflections obtained within the least squares method ($I > 2\sigma(I)$)	828/408/360	739/411/308	2025/278/199	1415/274/184	1429/278/249
Number of parameters in refinement	16				
Weighting scheme	1 / [$\sigma^2(F_0^2)$ + (0.0922P)^2 + 0.01P], $P = (F_0^2 + 2F_c^2) / 3$	1 / [$\sigma^2(F_0^2)$+(0.0891P)^2 + 0.01P], $P = (F_0^2 + 2F_c^2) / 3$	1 / [$\sigma^2(F_0^2)$ + (0.1029P)^2], $P = (F_0^2 + 2F_c^2) / 3$	1 / [$\sigma^2(F_0^2)$ + (0.1640P)^2], $P = (F_0^2 + 2F_c^2) / 3$	1 / [$\sigma^2(F_0^2)$ + (0.0767P)^2], $P = (F_0^2 + 2F_c^2) / 3$
R_1 ($I > 2\sigma(I)$)	0.0586	0.0644	0.0558	0.0954	0.0591
wR_2	0.1566	0.1616	0.1410	0.2259	0.1383
S	1.330	1.312	1.023	1.062	1.059
Program	SHELXL-97 [21]				

Table 3

Coordinates of atoms and their equivalent thermal parameters $U_{eq} \times 10^2$ (Å^2), site occupancies p (SOF) and main interatomic distances d (Å) in the structures of $PbMoO_4$ crystals according to the NDA and XDA data.

Technique	NDA		XDA		
Parameter	Sample				
	PMO-N_2	PMO-N_2(Pb)	PMO-A	PMO-N_2	PMO-N_2(Pb)
Pb (4a)					
x	1/2	1/2	1/2	1/2	1/2
y	3/4	3/4	3/4	3/4	3/4
z	1/8	1/8	1/8	1/8	1/8
p	0.2480(3)	0.2500(1)	0.2440(3)	0.2400(3)	0.2480(3)
U_{eq}	1.96(4)	1.90(4)	0.56(2)	0.692(9)	1.741(7)
Mo (4b)					
x	0	0	0	0	0
y	1/4	1/4	1/4	1/4	1/4
z	1/8	1/8	1/8	1/8	1/8
p	0.2500(2)	0.2500(2)	0.2500(2)	0.2500(2)	0.2480(3)
U_{eq}	1.77(4)	1.70(5)	0.30(4)	0.45(2)	1.49(2)
O (16f)					
x	0.2353(2)	0.2354(2)	−0.2356(9)	0.2338(8)	−0.2310(8)
y	0.3869(2)	0.3869(2)	0.1129(9)	0.3873(9)	0.3883(8)
z	0.04410(7)	0.04410(7)	0.0437(5)	0.0443(4)	0.0427(3)
p	0.997(4)	0.988(4)	1.00(1)	1.00(1)	1.00(1)
U_{eq}	2.26(4)	2.15(4)	0.86(9)	0.83(7)	2.23(9)
Pb–O $\times$ 4	2.6083(8)	2.6079(8)	2.603(6)	2.610(4)	2.611(4)
–O $\times$ 4	2.6294(9)	2.6292(9)	2.628(6)	2.629(5)	2.643(4)
[Pb–O]$_{avr}$	2.61885	2.61855	2.6155	2.6195	2.627
Mo–O $\times$ 4	1.7728(8)	1.7734(9)	1.776(6)	1.765(4)	1.770(4)

a stoichiometric deficiency of Pb^{2+} ions ($V_{Pb}^{n}{}'$), resulting in the formation of two defect states of Pb^{3+} and O^-, which act as color centers.

Structural features of the PTO crystals as well as the presence of chemical elements with several valence states in their composition result in the formation of various defect centers, including point defects and their associates, which significantly affect the functional properties of PTO crystals, and, consequently, their application. The presence of both native point defects and impurities in PTO structures is primarily determined by the growth and processing conditions. The purpose of our study was to establish the influence of growth atmosphere on the type and concentration of point defects in $PbTO_4$ (T = Mo, W) single crystals, grown by the Czochralski method.

2. Experimental technique

$PbMoO_4$ and $PbWO_4$ crystals with a diameter of 15–20 mm and a length of 180 mm were grown by the Czochralski method on the "Analogue" growth equipment, provided with a weight sensor, in the Pt crucible in the $\langle 001 \rangle$ direction in an air or nitrogen atmosphere followed by an annealing in vacuum. A ceramic technology was used to grow PTO crystals. Charges for PTO synthesis were prepared using extra pure grade PbO and WO_3 oxides and GR grade MoO_3 oxide (Sigma-Aldrich, USA) taken in a stoichiometric ratio or with an excess of PbO (Table 1). The temperature gradient, and rotation and pulling rates

were fixed for all crystals ($T_z = 50°/\text{cm}$; $\Omega = 20$ rpm; $V = 3$ mm/h). Crystallization front was flat or slightly convex. All the crystals were free of impurity phases and macroscale defects (gas bubbles and crystal cracking) and did not contain scattering centers. The conditions used to grow the crystals are described in detail in [11,17]. Photos of PTO crystals are given in [14,17].

The objects of the structural investigation were two $PbWO_4$ samples and three $PbMoO_4$ ones, grown in an air (PTO-A) and nitrogen (PTO-N_2) atmospheres and annealed in vacuum. All samples were grown from a stoichiometric mixture of the oxides, except for PMO-N_2(Pb) grown from the mixture with an excess of PbO (Table 1).

The X-ray powder diffraction data for samples ground to a powder (~100 mg) were collected in reflection mode at room temperature on HZG-4 (flat graphite monochromator) X-ray powder diffractometer using Cu K_α radiation and a diffracted beam (step-scan mode; the count time was 15 s and the step size was 0.02°) in the 2θ angle range of 15°–140°. To prevent any orientation predominating, the samples were rotated during X-ray data collection. The preliminary X-ray powder diffraction data processing was performed using the FullProf-2007 software package [18]. The qualitative phase analysis of the samples, which was performed with the use of the PCPDFWIN automatic search software for reading the PDF-2 database, showed that all samples were single phase. All calculations intended for refinement of the composition and structure of powder samples were performed by the Rietveld method (RM) with the DBWS-9411 program [19].

The X-ray Diffraction Analysis (XDA) of samples ~0.1 $\times$ 0.1 $\times$ 0.1 mm^3 in size was carried out on a STOE Stadi Vari PILATUS 100 K single-crystal diffractometer at room temperature (Mo K_α, $\lambda =$ 0.71073 Å, graphite monochromator). The preliminary X-ray diffraction data processing was carried out using the WinGX pack [20] with a correction for absorption (MULTISCAN).

Neutron Diffraction Analysis (NDA) of samples of ~5 $\times$ 5 $\times$ 5 mm^3 in size was carried out at room temperature on the four-circle single-crystal diffractometer installed at the hot source (5C2) of the Orphee reactor (LLB, France, $\lambda = 0.83$ Å).

The crystal structures of all samples were refined by the full-matrix least-squares method in the isotropic and anisotropic approximations for all atoms using the SHELXL-97 software package [21], taking into account the atomic scattering curves for neutral atoms. The technique described in detail in [22,23] was used for the refinement of crystal structures of the samples under investigation due to the correlation between site occupancies and thermal parameters.

3. Results and discussion

The unit cell parameter can be used as a structural parameter to qualitatively judge the composition of the crystals. Fig. 2 shows the unit cell parameters of the PTO crystals under investigation, determined for samples of various sizes by different diffraction methods: for crystals ground to a powder (~100 mg) — by the RM; for microparts of the same crystals (~0.1 $\times$ 0.1 $\times$ 0.1 mm^3) — by single-crystal XDA; and for macroparts of the same crystals (~5 $\times$ 5 $\times$ 5 mm^3) — by single-crystal

Table 4

Refined compositions of $PbMoO_4$ crystals determined by the NDA, XDA and RM.

Sample	Refined composition		
	NDA	XDA	RM
PMO-A	–	$(Pb_{0.976(1)}\square_{0.024})MoO_{4.00(3)}$	$(Pb_{0.993(2)}\square_{0.007})MoO_4$ $R_p = 9.71$ $R_{w-p} = 13.23$
PMO-N_2	$(Pb_{0.992(1)}\square_{0.008})MoO_{3.99(2)}$	$(Pb_{0.960(1)}\square_{0.040})MoO_{4.00(4)}$	$(Pb_{0.989(2)}\square_{0.011})MoO_4$ $R_p = 6.95$ $R_{w-p} = 9.35$
PMO-N_2(Pb)	$PbMo^{5.90(4)+}(O_{3.95(2)}\square_{0.05})$	$(Pb_{0.992(1)}\square_{0.008})(Mo_{0.992(1)}\square_{0.008})O_{4.00(4)}$	$Pb(Mo_{0.986(3)}\square_{0.014})O_4$ $R_p = 7.90$ $R_{w-p} = 10.75$

Table 5
Crystallographic data, experimental details and parameters of PbWO$_4$ crystal structure refinement according to the NDA and XDA data.

Chemical formula of the nominal composition	PbWO$_4$			
System, space group, Z	Tetragonal, $I4_1/a$, 4			
Technique	NDA		XDA	
Sample	PWO-A	PWO-N$_2$	PWO-A	PWO-N$_2$
a, Å	5.4637(1)	5.4609(2)	5.4612(4)	5.4579(5)
c, Å	12.0490(3)	12.0410(4)	12.020(1)	12.054(1)
V, Å^3	359.69(2)	359.08(2)	359.49(6)	359.07(6)
D_x, g/cm^3	8.403	8.418	8.431	8.417
Radiation λ, Å	0.828		Mo K_α; 0.71073	
Absorption μ, mm^{-1}	0.01		78.81	78.68
T, K	293			
Sample size, mm	~5 × 5 × 5		~0.1 × 0.1 × 0.1	
Diffractometer	5C2		STOE Stadi Vari PILATUS 100 K	
Type of scan	ω			
θ_{max}, deg.	42.315	42.82	30.815	35.615
Limits h, k, l	$-8 \leq h \leq 0$	$-8 \leq h \leq 8$	$-7 \leq h \leq 7$	$-8 \leq h \leq 8$
	$0 \leq k \leq 8$	$-8 \leq k \leq 8$	$-7 \leq k \leq 7$	$-8 \leq k \leq 8$
	$-19 \leq l \leq 5$	$0 \leq l \leq 19$	$-17 \leq l \leq 17$	$-11 \leq l \leq 19$
Number of reflections measured/number of unique reflections /number of reflections obtained within the least squares method ($I > 2\sigma(I)$)	650/404/312	683/416/333	4046/282/211	995/112/59
Number of parameters in refinement	16	16	16	16
Weighting scheme	$1 / [\sigma^2(F_0^2) + (0.1316P)^2 + 0.01P]$, $P = (F_0^2 + 2F_c^2) / 3$	$1 / [\sigma^2(F_0^2) + (0.0739P)^2 + 0.02P]$, $P = (F_0^2 + 2F_c^2) / 3$	$1 / [\sigma^2(F_0^2) + (0.1125P)^2]$, $P = (F_0^2 + 2F_c^2) / 3$	$1 / [\sigma^2(F_0^2) + (0.1573P)^2]$, $P = (F_0^2 + 2F_c^2) / 3$
R_1 ($I > 2\sigma(I)$)	0.0644	0.0596	0.0837	0.0928
wR_2	0.2120	0.1534	0.2132	0.2476
S	1.341	1.328	0.818	0.992
Program	SHELXL-97 [21]			

Table 6
Coordinates of atoms and their equivalent thermal parameters $U_{eq} \times 10^2$ ($\mathrm{Å}^2$), site occupancies p (SOF) and main interatomic distances d (Å) in the structures of $PbWO_4$ crystals according to the NDA and XDA data.

Technique	NDA		XDA	
Parameter	Sample			
	PWO-A	PWO-N_2	PWO-A	PWO-N_2
Pb ($4a$)				
x	1/2	1/2	1/2	1/2
y	3/4	3/4	3/4	3/4
z	1/8	1/8	1/8	1/8
p	0.2500(1)	0.2497(3)	0.2500(1)	0.2500(1)
U_{eq}	1.93(4)	2.36(5)	0.96(2)	0.77(3)
W ($4b$)				
x	0	0	0	0
y	1/4	1/4	1/4	1/4
z	1/8	1/8	1/8	1/8
p	0.2500(2)	0.2500(2)	0.2490(2)	0.2500(2)
U_{eq}	1.67(5)	2.07(6)	0.14(1)	0.50(3)
O ($16f$)				
x	−0.2333(2)	−0.2332(2)	−0.2369(5)	−0.235(1)
y	0.3906(2)	0.3908(2)	0.1033(6)	0.387(2)
z	0.04302(7)	0.04307(7)	0.0459(5)	0.0432(8)
p	0.980(3)	0.978(4)	0.9954(8)	0.964(2)
U_{eq}	2.19(4)	2.60(6)	1.19(7)	1.12(9)
Pb–O × 4	2.6085(9)	2.6110(9)	2.587(4)	2.598(9)
–O × 4	2.636(1)	2.637(1)	2.636(5)	2.646(9)
[Pb–O]$_{avr}$	2.62225	2.624	2.6115	2.622
W–O × 4	1.7853(9)	1.786(1)	1.795(4)	1.779(9)

NDA. According to Fig. 2, a qualitative agreement between the unit cell parameters, determined for various samples by different methods, is observed. The exception is PMO-N_2(Pb) sample, where the c unit cell parameters are clearly different (Fig. 2), that may be due to the bulk composition inhomogeneity of the PMO-N_2(Pb) crystal. It should be mentioned that the quantitative variation of the unit cell parameters

Table 7
Crystallographic data, coordinates of atoms and their equivalent or isotropic thermal parameters $U_{eq} \times 10^2$ ($\mathrm{Å}^2$), site occupancies p (SOF) and main interatomic distances d (Å) in the structure of PWO-A crystal refined in the framework of space group $I\bar{4}$ according to the XDA data.

Parameter	Value	Parameter		Value
Pb(1)		O(1)		
x	1/2	x		0.228(2)
y	0	y		−0.140(2)
z	1/4	z		0.082(1)
p	0.2475(18)	p		1.000[a]
U_{eq}	0.76(2)	U_{iso}		0.03(15)
Pb(2)		O(2)		
x	1/2	x		0.240(2)
y	1/2	y		0.364(2)
z	0	z		0.169(1)
p	0.2450(18)	p		1.000[a]
U_{eq}	0.54(2)	U_{iso}		0.54(18)
W(1)		Pb(1)	O(1) × 4	2.619(10)
x	0		O(2) × 4	2.632(12)
y	0	Pb(1)	O(1) × 4	2.655(11)
z	0		O(2) × 4	2.582(12)
p	0.2500(18)	W(1)	O(1) × 4	1.763(10)
U_{iso}	0.37(2)	W(2)	O(2) × 4	1.797(11)
W(2)		R_1 ($I > 2\sigma(I)$)		0.0668
x	0	wR_2		0.1324
y	1/2	S		0.660
z	1/4			
p	0.2475(18)			
U_{iso}	0.52(2)			

[a] Parameter was not refined.

may be due to the experimental conditions: different angular ranges, wavelengths, the number of diffraction reflections, scan mode, instrumental capabilities of experimental data collection, processing, and refinement [24].

It should be noted that the yellow coloration was observed for all the crystals under investigation, regardless of growth atmosphere, but with the same post-growth annealing in vacuum, except for gray-purple PMO-N_2(Pb) sample (Table 1). According to [25], the color of PTO crystals may be primarily associated with different formal charges of W and Mo ions, as well as with color centers, i.e., associates of point defects. In describing the results of refinement of crystal structures of the samples studied, we maintain the same position.

The results of PMO crystal structure refinement by the XDA, NDA and RM are given in Tables 2–4.

Analysis of the compositions of PMO-N_2 and PMO-N_2(Pb) crystals, as refined by the NDA (Table 4), shows an absence of vacancies in the Mo sites and vacancy presence in the O sites ($V_O^{n\bullet}$) for both samples and in the Pb sites ($V_{Pb}^{n'}$) for PMO-N_2 sample. These data together with the color of crystals (Tables 1, 4) and the electroneutrality condition allow the following quasi-chemical equations for these samples: $0 \rightarrow V_{Pb}^{n'} + V_O^{n\bullet}$ (Eq. (1)) or $0 \rightarrow V_{Pb}^{n'} + Pb_{Pb}^{n\bullet}$ ($Pb^{2+} \rightarrow Pb^{3+}$) taking into account the standard deviation of the O site occupancy (Eq. (2)) — for the light yellow PMO-N_2 sample with the refined composition $(Pb_{0.992(1)}\square_{0.008})MoO_{3.99(2)}$, and $0 \rightarrow nMo_{Mo'} + V_O^{n\bullet}$ ($Mo^{6+} \rightarrow Mo^{5+}$) (Eq. (3)) — for the gray-purple PMO-N_2(Pb) sample with the refined composition $PbMo^{5.90(4)+}(O_{3.95(2)}\square_{0.05})$. It should be noted that, according to [13], the purple color of complex scheelite crystals with general composition $(Na_{0.5}Gd_{0.5})MoO_4$ is due to the presence of Mo^{5+} ions. Therefore, based on our data, it can be concluded that the light yellow color of PMO crystals is due to the vacancies in the O and Pb sites that may be accompanied by the transition $Pb^{2+} \rightarrow Pb^{3+}$, while the gray-purple color of PMO-N_2(Pb) sample may result from the transition $Mo^{6+} \rightarrow Mo^{5+}$.

The unit cell parameters of PMO-N_2 and PMO-N_2(Pb) samples (Fig. 2) are in compliance with their refined compositions: increase in the unit cell parameters of PMO-N_2(Pb) sample due to the some Mo^{5+} ions content in the refined composition ($r_{Mo}^{5+} = 0.46$ Å, $r_{Mo}^{6+} = 0.41$ Å [26]) is compensated by a greater content of oxygen vacancies in this sample that results to the similar unit cell parameters for PMO-N_2(Pb) and PMO-N_2 samples (Tables 2, 4). The same increase in the unit cell parameters was observed for ZnO:K system [27].

Based on the compositions of PMO samples, refined by the XDA (Table 4), it can be established that the lower value of the c unit cell parameter of PMO-N_2(Pb) sample (Fig. 2) with the refined composition $(Pb_{0.992(1)}\square_{0.008})(Mo_{0.992(1)}\square_{0.008})O_{4.00(4)}$ can be due to the vacancies in the Mo sites. It is possible that the c unit cell parameter correlates with the composition of the tetrahedral sites, and electroneutrality of the system is being provided by "holes": $0 \rightarrow V_{Pb}^{n'} + V_{Mo}^{n'} + mh^\bullet$ (Eq. (4)) with possible formation of the associates $(V_{Mo}^{n'}, nh^\bullet)^x$ or/and $(V_{Pb}^{n'}, nh^\bullet)^x$. Self-compensation of electric charges for PMO-A and PMO-N_2 crystals can be performed in accordance with Eq. (5): $0 \rightarrow V_{Pb}^{n'} + nh^\bullet \rightarrow (V_{Pb}^{n'}, nh^\bullet)^x$.

The compositions of PMO samples, refined by the RM, are not contradictory to those refined by the NDA and XDA (Table 4). According to all methods, PMO-A and PMO-N_2 samples are characterized only by the Pb site vacancies, their content being greater in the sample grown in the nitrogen atmosphere as compared with the sample grown in the air.

The vacancies in the Mo sites in PMO-N_2(Pb) crystal were also revealed by both RM and XDA (Table 4).

Thus, according to the XDA and RM (Table 4), the growth atmosphere influences the composition of the PMO-A and PMO-N_2 crystals obtained: deficiency of dodecahedral sites is greater for the crystals grown in an inert atmosphere if compared with those grown in air atmosphere. According to all diffraction methods used, an excess of PbO in the initial charge composition results in the deficiency of the Mo sites and gray-purple color of the PMO-N_2(Pb) crystal.

Table 8
Refined compositions of PbWO$_4$ crystals determined by the NDA, XDA and RM.

Sample	Refined composition		
	NDA	XDA	RM
PWO-A	PbW(O$_{3.94(4)}$□$_{0.06}$)	Pb(W$_{0.996(1)}$□$_{0.004}$)(O$_{3.982(3)}$□$_{0.018}$) (sp.gr. $I4_1/a$) [Pb(1)$_{0.495(4)}$W(1)$_{0.500(4)}$] [(Pb(2)$_{0.490(4)}$W(2)$_{0.495(4)}$] [O(1)$_{1.995}$O(2)$_{1.975}$]^a (sp.gr.$I\bar{4}$)	PbW(O$_{3.992(9)}$□$_{0.008}$) R_p = 12.34 R_{w-p} = 16.87
PWO-N$_2$	Pb$_{0.999(1)}$W(O$_{3.93(4)}$□$_{0.07}$)	Pb(W$_{0.996(1)}$□$_{0.004}$)(O$_{3.855(3)}$□$_{0.145}$) (sp.gr. $I4_1/a$)	PbW(O$_{3.993(7)}$□$_{0.007}$) R_p = 10.25 R_{w-p} = 14.76

^{a} The composition of oxygen site was obtained based on the electroneutrality condition.

The results of PWO crystal structure refinement by the XDA, NDA and RM are given in Tables 5–8.

Based on the PWO sample compositions refined by the NDA (Table 8), PWO-A and PWO-N$_2$ crystals are characterized by high oxygen vacancy content that corresponds to the quasi-chemical reaction: $0 \rightarrow V_O^{n\bullet} + ne' \rightarrow (V_O^{n\bullet},ne')^\times$ — color center (Eq. (6)). In addition, the presence of vacancies in the O sites in PWO structures was also determined by the RM (Table 8). Hence, the light yellow color of PWO crystals is related primarily to the presence of oxygen vacancies in the structure.

The XDA of microparts of PWO-A and PWO-N$_2$ crystals revealed the presence of additional reflections (~50%) that cannot be indexed within the framework of space group $I4_1/a$ (00l with l = 2n, hk0 with h + k = 2n are not characteristic for space group $I4_1/a$). Selection of the space group $I\bar{4}$ from three possible space groups $I4/m$, $I4$ or $I\bar{4}$ based on the extinction law is due to the correspondence of regular system of points of space groups $I4_1/a$ and $I\bar{4}$. This effect was first found for PbWO$_4$ crystals and was not observed for PbMoO$_4$ ones (space group $I4_1/a$). Similar symmetry reduction from space group $I4_1/a$ to $I\bar{4}$ was revealed for the complex oxides with scheelite-like structures (Na$_{0.5}$Gd$_{0.5}$)WO$_4$:10Yb [28], (Li$_{0.5}$Yb$_{0.5}$)MoO$_4$ [29], (Na$_{0.5}$Bi$_{0.5}$)WO$_4$ [30], and the reduction to space group $P\bar{4}$ was found for (Na$_{0.5}$Gd$_{0.5}$)MoO$_4$:10Yb [31]. In case of PWO-A and PWO-N$_2$ crystals we may consider a kinetic phase transition of the order–disorder type [32,33], i.e. a partially ordered non-centrosymmetric phase (space group $I\bar{4}$) forms in the area of stability of the disordered centrosymmetric phase (space group $I4_1/a$). Analysis of the results of X-ray diffraction investigation of a large number of scheelite family crystals together with the conditions of their growth allows us to distinguish two distinctive features, technological and methodological, for such a phenomenon [31]. Primarily, such ordering may occur due to the presence of crystallographic sites co-occupied by several atoms, that is realized, for example, in the dodecahedral sites in scheelite-type structures [28-31] or by atoms and vacancies.

Indeed, the refinement (XDA) of crystal structures of PWO-A and PWO-N$_2$ microparts within the framework of the space group $I4_1/a$ indicates high deficiency of the O sites (it is also confirmed by the NDA), which is virtually absent in PbMoO$_4$ crystals (Table 4), that results in the distribution and ordering of oxygen vacancies over two crystallographic sites during the transition from the space group $I4_1/a$ to $I\bar{4}$: [Pb(1)$_{0.5}$W(1)$_{0.5}$][(Pb(2)$_{0.5}$W(2)$_{0.5}$][O(1)$_2$O(2)$_2$].

The refinement of the composition of PWO-A crystal (XDA) within the framework of space group $I4_1/a$ (total reflections read, 2034), accompanied by the splitting of 4-fold Pb and W sites and 8-fold O site (space group $I4_1/a$) into two 2-fold Pb and W sites and two 4-fold O sites (space group $I\bar{4}$) (total reflections read, 4046) (Fig. 1b), respectively, allows writing its composition as [Pb(1)$_{0.495(4)}$W(1)$_{0.500(4)}$] [(Pb(2)$_{0.490(4)}$W(2)$_{0.495(4)}$][O(1)$_{1.995}$O(2)$_{1.975}$] (Tables 7,8). Thermal parameters were refined in the anisotropic approximation for lead atoms and in isotropic one for all other atoms; site occupancies were refined for all cations. The O site occupancy was not refined due to its strong correlation with the thermal parameters; the composition of oxygen site

was obtained based on the electroneutrality condition. Further details of the crystal structure investigation may be obtained from FIZ Karlsruhe, 76,344 Eggenstein-Leopoldshafen, Germany (fax: (+49)7247-808-666; e-mail: crysdata@fiz-karlsruhe.de, on quoting the deposition number CSD-430833.

At room temperature the bandgap in PbMoO$_4$ (3.22 eV) is higher than that in PbWO$_4$ (3.82 eV) [2], that indicates the higher portion of covalent bond in PbWO$_4$ as compared with that in PbMoO$_4$, and, consequently, differences in their properties (e.g., in their melting points, t_{MP}(PbMoO$_4$) = 1050 °C and t_{MP}(PbWO$_4$) = 1123 °C), and symmetry, as it was shown in the present study.

Different symmetry of scheelite-like molybdates and tungstates was found for complex oxides with general composition CaGd$_{2(1-x)}$Eu$_{2x}$(MoO$_4$)$_{4(1-y)}$(WO$_4$)$_{4y}$ ($0 \leq x \leq 1$, $0 \leq y \leq 1$) by a combination of transmission electron microscopy techniques and X-ray powder diffraction [34]. Morozov et al. [34] revealed that a solid solutions with y = 0 (molybdates) have (3 + 2)D incommensurately modulated structures and crystallize in the superspace group $I4_1/a(\alpha,\beta,0)00(-\beta,\alpha,0)00$, while the structures with y = 1 (tungstates) are (3 + 1)D incommensurately modulated with superspace group $I2/b(\alpha\beta0)00$. Rietveld refinement of CaGd$_{2-x}$(WO$_4$)$_4$:Er^{3+}/Yb^{3+} and CaLa$_{2-x}$(MoO$_4$)$_4$:Ho^{3+}/Yb^{3+} crystal structures also found them to be modulated [35,36].

Therefore, a general trend for scheelite-like tungstates and molybdates was revealed: the possibility of appearance of different symmetry, and, hence, the fundamentally different properties can be expected for PTO crystals as has been shown in a number of publications.

Appendix A. Supplementary data

Supplementary data to this article can be found online at http://dx.doi.org/10.1016/j.matdes.2016.02.062.

References

[1] A.W. Sleight, Accurate cell dimensions for ABO$_4$ molybdates and tungstates, Acta Crystallogr. B 28 (1972) 2899–2902.
[2] G.A. Coquin, D.A. Pinnow, A.W. Warner, Physical properties of lead molybdate relevant to acousto-optic device applications, J. Appl. Phys. 42 (6) (1971) 2162–2168.
[3] A. Borisevich, A. Fedorov, A. Hofstaetter, M. Korzhik, B.K. Meyer, O. Missevitch, R. Novotny, Lead tungstate scintillation crystal with increased light yield for the PANDA electromagnetic calorimeter, Nucl. Inst. Methods A 537 (2005) 101–104.
[4] F.A. Danevich, B.V. Grinyov, S. Henry, M.B. Kosmyna, H. Kraus, et al., Feasibility study of PbWO$_4$ and PbMoO$_4$ crystal scintillators for cryogenic rare events experiments, Nucl. Inst. Methods A 622 (2010) 608–613.

[5] S. Pirro, J.W. Beeman, S. Capelli, M. Pavan, E. Previtali, P. Gorla, Scintillating double-beta-decay bolometers, Phys. At. Nucl. 69 (2006) 2109.

[6] L.L. Nagornaya, F.A. Danevich, A.M. Dubovik, B.V. Grinyov, S. Henry, et al., Oxide scintillators to search for dark matter and double beta decay, IEEE Trans. Nucl. Sci. 56 (2009) 2513–2516.

[7] E.N. Galashov, P.S. Galkin, P.E. Plusnin, V.N. Shlegel, Specific features of the phase formation, synthesis, and growth of $ZnMoO_4$ crystals, Crystallogr. Rep. 59 (2) (2014) 288–290.

[8] L. Bergé, R.S. Boiko, M. Chapellier, et al., Purification of molybdenum, growth and characterization of medium volume $ZnMoO_4$ crystals for the LUMINEU program, J. Instrum. 9 (2014), P06004.

[9] E.N. Galashov, V.V. Atuchin, A.S. Kozhukhov, L.D. Pokrovsky, V.N. Shlegel, Growth of $CdWO_4$ crystals by the low thermal gradient Czochralski technique and the properties of a (010) cleaved surface, J. Cryst. Growth 401 (2014) 156–159.

[10] T.M. Bochkova, M.D. Volnyanskii, D.M. Volnyanskii, V.S. Shchetinkin, Color centers in lead molybdate crystals, Phys. Solid State 45 (2) (2003) 244–247.

[11] T.T. Basiev, V.N. Baumer, Yu.N. Gorobets, M.E. Doroshenko, M.B. Kosmyna, Peculiarities of the growth of $PbWO_4:Nd^{3+}$ and $PbMoO_4:Nd^{3+}$ single crystals, Crystallogr. Rep. 54 (4) (2009) 697–701.

[12] S. Takano, S. Esahi, K. Mori, T. Namikata, Growth of high-quality single crystals of lead molybdate, J. Cryst. Growth 24 (25) (1974) 437–440.

[13] G.M. Kuz'micheva, V.B. Rybakov, K.A. Subbotin, et al., Colors of mixed-substituted double molybdate single crystals having scheelite structure, Russ. J. Inorg. Chem. 57 (2012) 1128–1133.

[14] Yu.N. Gorobets, I.A. Kaurova, G.M. Kuz'micheva, A.N. Shekhovtsov, V.B. Rybakov, A. Cousson, Influence of the dopant type on point defects in $PbMoO_4$ crystals, J. Surf. Investig. 8 (4) (2014) 734–744.

[15] R. Oeder, A. Scharmann, D. Schwabe, B. Vitt, Growth and properties of $PbWO_4$ and $Pb(WO_4)$-(MoO_4) mixed crystals, J. Cryst. Growth 43 (1978) 537–540.

[16] T.H. Kim, Sh. Cho, K. Lee, M.S. Jang, J.H. Ro, Influence of crystal growth atmosphere on the formation of color centers in $PbWO_4$ single crystals, Appl. Phys. Lett. 81 (20) (2002) 3756–3758.

[17] M.B. Kosmyna, B.P. Nazarenko, V.M. Puzikov, A.N. Shekhovtsov, Development of growth technologies for the photonic single crystals by the Czochralski method at Institute for Single Crystals, NAS of Ukraine, Acta Phys. Polon. A 124 (2) (2013) 305–313.

[18] J. Rodriges-Carvajal, The programs for Rietveld refinement, Physica B 192 (1993) 55–69.

[19] R.A. Young, A. Sakthivel, T.S. Moss, C.O. Paiva-Santos, Rietveld analysis of X-Ray and neutron powder diffraction patterns, User's Guide to Program DBWS-9411, March 30 1995.

[20] L.J. Farrugia, WinGX suite for small-molecule single-crystal crystallography, J. Appl. Crystallogr. 32 (1999) 837–838.

[21] G.M. Sheldrick, A short history of SHELX, Acta Crystallogr. A64 (2008) 112–122.

[22] T.I. Mel'nikova, G.M. Kuz'micheva, N.B. Bolotina, V.B. Rybakov, Ya.V. Zubavichus, et al., Structural features of compounds of the sillenite family, Crystallogr. Rep. 59 (3) (2014) 353–361.

[23] T.I. Mel'nikova, G.M. Kuz'micheva, N.B. Bolotina, N.V. Sadovskaya, Development of methods of X-ray diffraction analysis for determining the composition and structure of sillenite-family crystals, Crystallogr. Rep. 59 (2) (2014) 155–159.

[24] E.A. Tyunina, I.A. Kaurova, G.M. Kuz'micheva, V.B. Rybakov, A. Cousson, O. Zaharko, Diffraction methods for determination of composition and structural parameters of langasite family compounds, Vestn. MITHT 5 (1) (2010) 57–68 (Fine Chemical Technol.).

[25] Yu.S. Kuzminov, The color of oxide crystals as a characteristic of defect structure, in: Yu.S. Kuzminov (Ed.)Trudy GPI RAS: Physical and Chemical Aspects of Technology of Single Crystals of Complex Oxide Compounds, 64 2008, pp. 118–126 (in Russian).

[26] R.D. Shannon, Revised effective ionic radii and systematic studies of interatomic distances in halides and chalcogenides, Acta Crystallogr. A32 (6) (1976) 751–767.

[27] X. Si, Y. Liu, X. Wu, W. Lei, J. Xu, W. Du, T. Zhou, J. Lin, The interaction between oxygen vacancies and doping atoms in ZnO, Mater. Des. 87 (2015) 969–973.

[28] G.M. Kuz'micheva, V.B. Rybakov, V.L. Panyutin, E.V. Zharikov, K.A. Subbotin, Symmetry of $(Na_{0.5}R_{0.5})MO_4$ crystals (R = Gd, La; M = W, Mo), Russ. J. Inorg. Chem. 55 (9) (2010) 1448–1453.

[29] V. Volkov, C. Cascales, A. Kling, C. Zaldo, Growth, structure, and evaluation of laser properties of $LiYb(MoO_4)_2$ single crystal, Chem. Mater. 17 (2005) 291–300.

[30] J. Hanuza, A. Benzar, A. Haznar, M. Maczka, A. Pietraszko, J.H. van der Maas, Structure and vibrational dynamics of tetragonal $NaBi(WO_4)_2$ scheelite crystal, Vib. Spectrosc. 12 (1996) 25–36.

[31] G.M. Kuz'micheva, I.A. Kaurova, E.A. Zagorul'ko, N.B. Bolotina, V.B. Rybakov, A.A. Brykovskiy, E.V. Zharikov, D.A. Lis, K.A. Subbotin, Structural perfection of the $(Na_{0.5}Gd_{0.5})MoO_4:Yb$ laser crystal, Acta Mater. 87 (2015) 25–33.

[32] A. Putnis, J.D.C. McConnell, Principles of Mineral Behaviour, Blackwell, Oxford, 1980.

[33] A.G. Shtukenberg, Yu.O. Punin, O.V. Frank-Kamenetskaya, The kinetic ordering and growth dissymmetrisation in crystalline solid solutions, Russ. Chem. Rev. 75 (12) (2006) 1083–1106.

[34] V.A. Morozov, A. Bertha, K.W. Meert, S. Van Rompaey, D. Batuk, G.T. Martinez, S. Van Aert, P.F. Smet, M.V. Raskina, D. Poelman, A.M. Abakumov, J. Hadermann, Incommensurate modulation and luminescence in the $CaGd_{2(1-x)}Eu_{2x}(MoO_4)_{4(1-y)}(WO_4)_{4y}$ $(0 \leq x \leq 1, 0 \leq y \leq 1)$ red phosphors, Chem. Mater. 25 (21) (2013) 4387–4395.

[35] C.S. Lim, A. Aleksandrovsky, M. Molokeev, A. Oreshonkov, V. Atuchin, The modulated structure and frequency upconversion properties of $CaLa_2(MoO_4)_4:Ho^{3+}/Yb^{3+}$ phosphors prepared by microwave synthesis, Phys. Chem. Chem. Phys. 17 (2015) 19278–19287.

[36] C.S. Lim, A. Aleksandrovsky, M. Molokeev, A. Oreshonkov, V. Atuchin, Microwave sol–gel synthesis and upconversion photoluminescence properties of $CaGd_2(WO_4)_4:Er^{3+}/Yb^{3+}$ phosphors with incommensurately modulated structure, J. Solid State Chem. 228 (2015) 160–166.